

# Radio-Frequency Manipulation of Fano-Feshbach Resonances in an Ultracold Fermi Gas of $^{40}\text{K}$

Lianghui Huang<sup>1</sup>, Pengjun Wang<sup>1</sup>, B. P. Ruzic<sup>2</sup>, Zhengkun Fu<sup>1</sup>,  
Zengming Meng<sup>1</sup>, Peng Peng<sup>1</sup>, J. L. Bohn<sup>2</sup> and Jing Zhang<sup>1,3†</sup>

<sup>1</sup>*State Key Laboratory of Quantum Optics and Quantum Optics Devices,  
Institute of Opto-Electronics, Shanxi University, Taiyuan 030006, P. R. China*

<sup>2</sup>*JILA, University of Colorado and National Institute of Standards and Technology, Boulder, Colorado 80309-0440, USA*

<sup>3</sup>*Synergetic Innovation Center of Quantum Information and Quantum Physics,  
University of Science and Technology of China, Hefei, Anhui 230026, P. R. China*

(Dated: June 18, 2021)

Experimental control of magnetic Fano-Feshbach resonances in ultracold  $^{40}\text{K}$  Fermi gases, using radio-frequency (RF) fields, is demonstrated. Spectroscopic measurements are made of three molecular levels within 50 MHz of the atomic continuum, along with their variation with magnetic field. Modifying the scattering properties by an RF field is shown by measuring the loss profile versus magnetic field. This work provides the high accuracy locations of ground molecular states near the s-wave Fano-Feshbach resonance, which can be used to study the crossover regime from a Bose-Einstein condensate to a Bardeen-Cooper-Schrieffer superfluid in presence of an RF field.

PACS numbers: 05.30.Fk, 03.75.Hh, 03.75.Ss, 67.85.-d

The capability to tune the strength of elastic interparticle interactions has led to explosive progress of using ultracold atomic gases to create and explore many-body quantum systems [1]. Magnetic-field-induced Fano-Feshbach resonances are among the most powerful tools for this purpose, and have been used widely in atomic gases of alkali atoms. An alternative technique for tuning interatomic interactions is called optical Feshbach resonances (OFR) [2, 3], in which free atom pairs are coupled to an electronically excited molecular state by a laser field tuned near a photoassociation resonance [4–7]. The OFR offers more flexible control over interaction strength with high spatial and temporal resolution. Furthermore, laser light in combination with magnetic Fano-Feshbach resonances have been developed to modify the interatomic interaction in Bose gases [8–10] and Fermi gases [11].

Radio-frequency (RF) radiation is an appealing alternative means for manipulating ultracold atoms. Note that for alkali atoms, magnetic field Fano-Feshbach resonances may be difficult to find, such as in  $^{87}\text{Rb}$ ; and that OFR's are problematic in these species because of large losses due to spontaneous emission. Manipulation of scattering lengths via RF radiation therefore represents a powerful new tool. In the context of ultracold gases, RF can be used to couple a two-atom scattering state to a bound molecular state (free-bound coupling) similarly to the OFR. RF also can drive transitions between bound states (bound-bound coupling). As a probe, RF has been used extensively to determine the s-wave scattering length near a Feshbach resonance by directly measuring the RF shift induced by mean-field interactions [12], to demonstrate many-body effects and quantum unitarity [13], and to probe the occupied spectral function of single-particle states and the energy dispersion through Bose-Einstein condensate (BEC) - Bardeen-

Cooper-Schrieffer (BCS) crossover [14]. RF can also be considered as a means of controlling scattering length in a variety of scenarios. Zhang et al. [15] proposed to independently control different scattering lengths in multicomponent gases using RF dressing. The RF coupling of magnetic Fano-Feshbach resonances in a  $^{87}\text{Rb}$  Bose gas has been studied experimentally and theoretically [16, 17]. Tscherbul et al. [18] performed a theoretical analysis of manipulating Feshbach resonances of  $^{87}\text{Rb}$  with RF field. Papoular et al. [19] suggested using a microwave field to control collisions in atom gases at zero magnetic field. Further, Avdeenkova [20] applied this same idea to manipulate scattering of polar molecules.

In this paper, we experimentally investigate a magnetic Fano-Feshbach resonance in combination with an RF field in ultracold  $^{40}\text{K}$  Fermi gases. We measure the spectrum of the nearby molecular bound states with partial-wave quantum number  $L = 0$  by applying a near-resonant RF field. We also measure the free-to-bound transition from free atoms with attractive interaction to these same molecular states. For all three states measured, the binding energies are in good agreement with a theoretical calculation. Further, the loss of atoms versus magnetic field is measured, to determine the ability of the RF field to modify scattering. The position of the narrow loss features induced by the RF field in the broad loss profile of magnetic Fano-Feshbach resonances can be changed easily by setting the frequency of RF field, which represents the modification of the scattering properties near a magnetic Fano-Feshbach resonance, producing resonance features narrower in magnetic field than the original resonance.

We consider potassium 40 atoms in a mixture of hyperfine states  $|F, M_F\rangle = |9/2, -9/2\rangle$  and  $|9/2, -7/2\rangle$ , where  $F$  and  $M_F$  are the total (electronic plus nuclear)

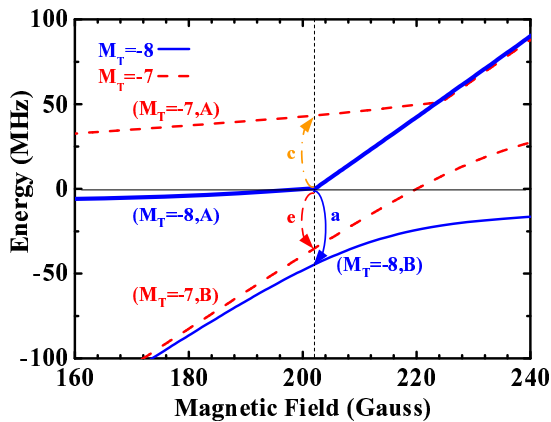


FIG. 1: (Color online) Energy spectrum of relevant molecular levels of  $^{40}\text{K}_2$  versus the magnetic field in the electronic ground state. The zero of energy is taken to be that of two separated atoms  $|9/2, -9/2\rangle + |9/2, -7/2\rangle$  at each magnetic field strength.  $M_T$  is total angular momentum projection  $M_{F_1} + M_{F_2}$

spin and its projection on the magnetic field axis, respectively. Atoms in such a mixture are known to have an s-wave Fano-Feshbach resonance at a magnetic field  $B = 202.2$  G [1]. We consider interspecies collisions between these two states, and their nearby molecular bound states, given in the atom-pair quantum numbers  $|F_1, M_{F_1}\rangle|F_2, M_{F_2}\rangle|L, M_L\rangle$ , as described in Hund's coupling case (e). Here  $L$  and  $M_L$  are the quantum numbers of the partial wave angular momentum and its projection. In an ultracold gas, the atoms start in either free pairs with  $L = 0$ , or else in a very weakly-bound Feshbach molecular state with  $L = 0$ . Since we consider only RF transitions that cannot change  $L$ , we omit this index in what follows.

Figure 1 shows the nearby bound s-wave ( $L = 0$ ) molecular levels versus magnetic field, as calculated by a coupled channel model. This model has been engineered to fit simultaneously the s-wave and p-wave Fano-Feshbach resonances reported in Ref. [27], and should be a reasonable representation of potassium cold collisions near  $B = 200$  Gauss. In this figure the zero of energy corresponds to the threshold energy of the entrance channel  $|9/2, -9/2\rangle + |9/2, -7/2\rangle$ . The figure shows two molecular bound states with total angular momentum projection  $M_T \equiv M_{F_1} + M_{F_2} = -8$  (blue solid lines), which exhibit an avoided crossing at the resonance. In the upper curve ( $M_T = -8, A$ ), the line represents the Feshbach molecule state for  $B < B_0$ , whereas it becomes a scattering resonance at  $B > B_0$ . The lower curve ( $M_T = -8, B$ ) remains a relatively deeply bound (by  $\sim 45$  MHz) state in the field range shown. These states can be reached by RF radiation polarized with the magnetic field along the quantization axis set by the magnetic field, satisfying the selection rule  $\Delta M_T = 0$ . In addition, the fig-

ure shows two bound states with  $M_T = -7$ , which can be reached by RF with perpendicular polarization, with selection rule  $\Delta M_T = \pm 1$ . The upper ( $M_T = -7, A$ ) of these bound states is weakly bound with respect to the  $|9/2, -9/2\rangle + |7/2, -7/2\rangle$  threshold, and becomes unbound into this continuum at  $B \approx 220$  Gauss. The figure also shows arrows (labeled a, c, e) indicating the allowed bound-to-bound transitions that are measured in the experiment.

The experimental apparatus has been described in our previous work [21–24]. The degenerate Fermi gas of about  $N \simeq 2 \times 10^6$   $^{40}\text{K}$  atoms in the  $|9/2, 9/2\rangle$  internal state is obtained with  $T/T_F \simeq 0.3$  by evaporatively sympathetic cooling with bosonic  $^{87}\text{Rb}$  atoms in the  $|2, 2\rangle$  state inside a crossed optical trap. Here  $T$  is the temperature and  $T_F$  is the Fermi temperature defined by  $T_F = E_F/k_B = (6N)^{1/3}\hbar\bar{\omega}/k_B$  with a geometric mean trapping frequency  $\bar{\omega}$ . Then Fermi gas with equal spin-population in the  $|9/2, -9/2\rangle$  and  $|9/2, -7/2\rangle$  states is prepared at about  $B \simeq 219.4$  G. These two hyperfine states form the incoming state  $|9/2, -9/2\rangle + |9/2, -7/2\rangle$  in the entrance channel for a pair of atoms, as shown in Fig. 1. We use a magnetically controlled Fano-Feshbach resonance at  $B_0 = 202.20 \pm 0.02$  G to adiabatically convert a pair of atoms into extremely weakly bound molecules (binding energy  $< 100$  kHz).

We place the coil just outside the glass cell and the oscillating magnetic field generated by the RF coil may be parallel (or perpendicular by changing the positions of the RF coil) to the magnetic bias field of the Fano-Feshbach resonance. We apply the RF pulse in a rectangular temporal shape, with variable time that depends on the measurement being made. Near resonance with one of the bound-to-bound transitions, the RF field induces loss in the population of Feshbach molecules due to the excitation to the other molecular states. In order to determine the number of remaining Feshbach molecules in the trap, after turning off the RF, another gaussian-shape RF pulse with duration about  $400 \mu\text{s}$  is applied to dissociate the remaining molecules into free atoms in the state  $|9/2, -9/2\rangle + |9/2, -5/2\rangle$ . The frequency of the RF pulse used to dissociate Feshbach molecules is fixed to a value that is about  $E_b$  kHz larger than the Zeeman splitting between the hyperfine states  $|9/2, -7/2\rangle$  and  $|9/2, -5/2\rangle$  for the certain magnetic field, which corresponds to the transition from the bound molecules to the free atom state  $|9/2, -9/2\rangle + |9/2, -5/2\rangle$ . After the dissociation RF pulse, we abruptly turn off the optical trap and magnetic field, and let the atoms ballistically expand for 12 ms in a magnetic field gradient applied along the  $\hat{y}$  axis and then take absorption image along the  $\hat{z}$  direction. The atoms in different hyperfine states  $N_\sigma$  ( $\sigma = |-7/2\rangle, |-5/2\rangle, \dots$ ) are spatially separated and analyzed, from which we determine the fraction  $N_{-5/2}/(N_{-5/2} + N_{-7/2})$  for different RF frequencies to obtain the spectrum of the bound molecular states.

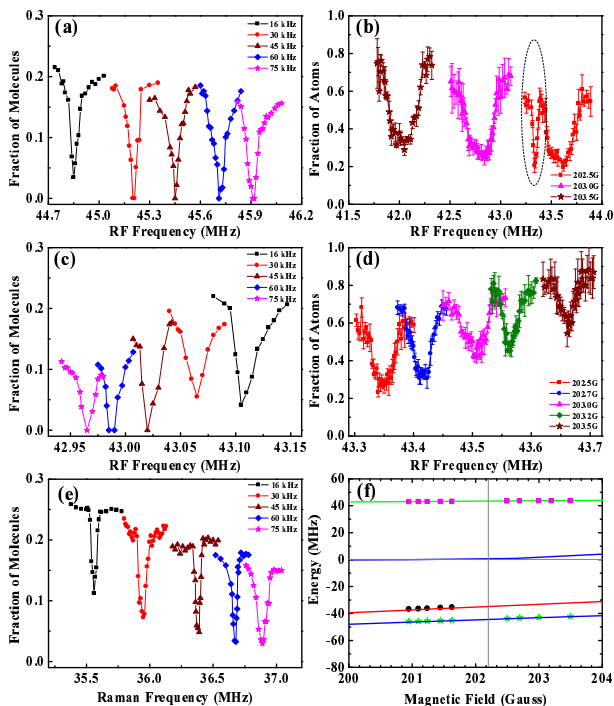


FIG. 2: (Color online) Bound-to-bound and free-to-bound spectroscopy of ground  $^{40}\text{K}_2$  molecules for different magnetic field. (a) The bound-to-bound spectroscopy from Feshbach molecular state to deeply bound molecular state ( $M_T = -8, B$ ). (b) The free-to-bound spectroscopy from free atom to deeply bound molecular state ( $M_T = -8, B$ ). (c) The bound-to-bound spectroscopy from Feshbach molecular state to deeply bound molecular state ( $M_T = -7, A$ ). (d) The free-to-bound spectroscopy from free atom to deeply bound molecular state ( $M_T = -7, A$ ). (e) The bound-to-bound spectroscopy of deeply bound molecular state ( $M_T = -7, B$ ) for different magnetic field, which is obtained by two-color stimulated Raman process. (f) The energies of deeply bound molecular state as the function of magnetic field are obtained from (a)-(e). The dot points are the experimental data and the solid lines are obtained from theoretical calculation.

Figure 2 reports the results of the spectroscopic measurements for the transitions described in Fig. 1. Figure 2(a) shows the bound-to-bound transition (labeled as "a" in Fig. 1) near 45 MHz for different magnetic fields corresponding to different binding energies  $E_b$  of the Feshbach molecules. Here the bound molecules are illuminated with the RF pulse duration time of 5 ms and the RF field is parallel to the direction of the magnetic bias field. The lifetimes of deeply bound molecular states are measured to be less than 2 ms, which are much shorter than the lifetimes of Feshbach molecules. When the RF field is perpendicular to the direction of the magnetic bias field, we do not observe any loss of the Feshbach molecules, confirming that the bound state is a state of  $M_T = -8$ . It is also possible to measure this state starting from a pair of free atoms at  $B > B_0$ , as shown in Fig. 2(b). Here the free atoms are illuminated with the

RF pulse duration time of 50 ms. From these data, we reproduce the binding energy of this state versus magnetic field, which is plotted as the lower data set in Fig. 2(f), and compared directly to the theoretical calculation (blue line).

Figure 2(c) shows the bound-to-bound transition (labeled as "c" in Fig. 1) near 43 MHz for different magnetic fields, corresponding to the transition from Feshbach molecular state to the upper branch molecular state ( $M_T = -7, A$ ). Again this transition is identified by the energetics of the transition and the slope of transition energy with respect to magnetic field, as computed in the model. The transition can be driven, as expected, by RF radiation of perpendicular polarization, exploiting the selection rule  $\Delta M_T = -1$ . We also note, to our surprise, that resonant features appear at the same transition frequencies for parallel polarization, with selection rule  $\Delta M_T = 0$ . The model is unable to identify such a state in the spectrum, and the appearance of these lines in parallel polarization remains a mystery. This state can also be identified in free-to-bound spectroscopy for magnetic fields above  $B_0 = 202.2$  G, Fig. 2(d). Comparing with the theoretical calculation, the measured bound-to-bound (free-to-bound) transition corresponds to the transitions near 43 MHz from Feshbach molecular state (free atoms) to the upper branch molecular state ( $M_T = -7, A$ ) as shown in the upper data set in Fig. 2(f). Note that the resonant position (43.35 MHz) of the free-to-bound spectra for the magnetic bias field 202.5 G in Fig. 2(d) corresponds to the narrow dip in Fig. 2(b) with the same magnetic bias field, since both transitions are nearly degenerate at this field.

We have also identified the lower branch molecular state ( $M_T = -7, B$ ). However, we can not observe this state via loss of the Feshbach molecules, even when applying the maximum power of RF field in our experimental setup, either in perpendicular or parallel polarization. This is presumably because of a comparatively small Franck-Condon overlap between the states. However, one can use a pair of laser beams to coherently couple two bound molecular states via a common electronically excited molecular state (two-color stimulated Raman process) to enhance the coupling between two ground bound-bound molecular states. Here, we carefully choose the one photon detuning of the Raman lasers (wavelength 772.4 nm) to avoid loss due to a Feshbach resonance induced by the laser between the ground Feshbach molecular state and the electronically excited molecular state [11, 25]. The configuration of the two Raman lasers has been described in our previous work [26]. Using these Raman lasers we measure bound-to-bound spectroscopy for ground  $^{40}\text{K}_2$  molecules near 36 MHz for different magnetic fields, as shown in Fig. 2(e). These binding energies are again in good agreement with the theoretical model, as shown by the red line in Fig. 2(f).

We now consider how the Fano-Feshbach resonance is

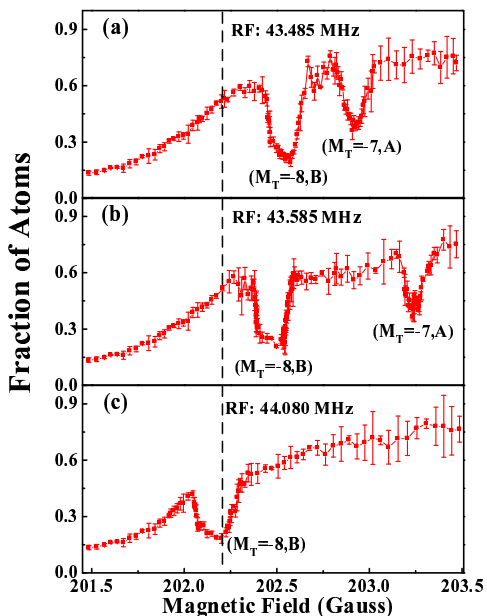


FIG. 3: (Color online) Atom loss from the entrance channel  $|9/2, -9/2\rangle, |9/2, -7/2\rangle$  in the vicinity of the Feshbach resonance 202.2 G for different frequencies of RF field. (a) The frequency of RF field is 43.485 MHz. (b) 43.585 MHz. (c) 44.080 MHz.

modified in the presence of the RF field. We do this by measuring the loss profile versus magnetic field, for various RF couplings. Two spin mixture states  $|9/2, -9/2\rangle$  and  $|9/2, -7/2\rangle$  are initially prepared at the magnetic field of 210 G and then the field is ramped quickly to its final value within 3 ms. Then the atoms are illuminated with the RF pulse for 50 ms with the RF field polarized parallel to the direction of the magnetic bias field. After this, the fraction of Feshbach molecules remaining is counted as above.

The resulting loss profiles as functions of the magnetic field for the different RF frequencies are shown in Fig. 3. The broad  $s$ -wave Fano-Feshbach resonance of two spin mixture states  $|9/2, -9/2\rangle$  and  $|9/2, -7/2\rangle$  is at  $B_0 = 202.2$  G (vertical dashed line in the figure) with a width of 7.04 G [27]. The maximum atom loss is not centered on this resonance, but rather occurs at lower-field regions of the spectrum (the BEC side of resonance), regardless of the RF frequency. Thus the main loss occurs where the Feshbach molecular state is already quite deeply bound [28–30] in sharp contrast with the bosonic case, where maximum loss is observed primarily on the resonance [31–33]. In addition, there are narrow loss features in the broad loss profile when the RF field is applied, which we attribute to transitions "a" and "c" in Figure 1, namely, transitions to the bound states ( $M_T = -8, B$ ) and ( $M_T = -7, A$ ). The former moves to lower magnetic fields as the RF frequency is increased, while the latter moves to higher magnetic field, as de-

scribed by the energies of these resonances. At an RF frequency of 44.080 MHz, the "a" transition coincides in magnetic field with the initial resonance, at  $B = 202.2$  G. In this case the naturally occurring magnetic Fano-Feshbach resonance and the RF-coupled bound state can interfere with one another. The profile of the scattering length can be deduced from the loss profile. Thus this shows that RF radiation may be used to place narrow resonances at any desired magnetic field (which means to locate on a desired position on a broad magnetic Fano-Feshbach resonance), opening new prospects for control of collisions. Moreover, our experimental scheme may be modified with the two optical fields coupling two ground molecular states through an excited molecular state. The dark molecular state generated by this protocol can be used to control the interaction strength near a magnetic Feshbach resonance, and suppress spontaneous emission by quantum interference [34].

In conclusion, we have experimentally demonstrated the technology of tuning a magnetic-field Fano-Feshbach resonance using an RF field in ultracold atomic Fermi gases. The spectrum of the nearby molecular states with partial-wave quantum number  $L = 0$  is measured by applying an RF field near the  $s$ -wave Fano-Feshbach resonance. By comparing to a theoretical calculation, we have identified the quantum numbers of the molecular states. We have moreover characterized the loss profile of the Fano-Feshbach resonance in the presence of the RF field. Since RF radiation is easily manipulated, this technology could be used to switch scattering lengths rapidly and precisely. The tunability of interatomic interactions, as demonstrated in this work, provides a new way to explore the fascinating quantum many-body system of strongly interacting Fermi gases.

This research is supported by the National Basic Research Program of China (Grant No. 2011CB921601), NSFC (Grant No. 11234008, 11361161002), NSFC Project for Excellent Research Team (Grant No. 61121064), and Doctoral Program Foundation of the Ministry of Education China (Grant No. 20111401130001). BPR and JLB acknowledge funding from an AFOSR MURI grant.

<sup>†</sup>Correspondence should be addressed to Jing Zhang (jzhang74@aliyun.com, jzhang74@sxu.edu.cn).

- 
- [1] C. Chin, R. Grimm, P. Julienne, and E. Tiesinga, *Rev. Mod. Phys.* **82**, 1225 (2010).
  - [2] P. O. Fedichev, Yu. Kagan, G. V. Shlyapnikov, and J. T. M. Walraven, *Phys. Rev. Lett.* **77**, 2913 (1996).
  - [3] J. L. Bohn and P. S. Julienne, *Phys. Rev. A* **60**, 414 (1999).
  - [4] K. Enomoto, K. Kasa, M. Kitagawa, and Y. Takahashi, *Phys. Rev. Lett.*, **101**, 203201 (2008).
  - [5] R. Yamazaki, S. Taie, S. Sugawa, and Y. Takahashi,

- Phys. Rev. Lett. **105**, 050405 (2010).
- [6] S. Blatt, T. L. Nicholson, B. J. Bloom, J. R. Williams, J. W. Thomsen, P. S. Julienne, and J. Ye, Phys. Rev. Lett. **107**, 073202 (2011).
- [7] M. Yan, B. J. DeSalvo, B. Ramachandhran, H. Pu, and T. C. Killian, Phys. Rev. Lett. **110**, 123201 (2013).
- [8] M. Junker, D. Dries, C. Welford, J. Hitchcock, Y. P. Chen, and R. G. Hulet, Phys. Rev. Lett. **101**, 060406 (2008).
- [9] D. M. Bauer, M. Lettner, C. Vo, G. Rempe, and S. Durr, Nature Phys. **5**, 339 (2009).
- [10] D. M. Bauer, M. Lettner, C. Vo, G. Rempe, and S. Durr, Phys. Rev. A **79**, 062713 (2009).
- [11] Z. Fu, P. Wang, L. Huang, Z. Meng, H. Hu, and J. Zhang, Phys. Rev. A **88**, 041601 (2013).
- [12] C. A. Regal and D. S. Jin, Phys. Rev. Lett. **90**, 230404 (2003).
- [13] S. Gupta, Z. Hadzibabic, M. W. Zwierlein, C. A. Stan, K. Dieckmann, C. H. Schunck, E. G. M. van Kempen, B. J. Verhaar, and W. Ketterle, Science **300**, 1723 (2003).
- [14] J. T. Stewart, J. P. Gaebler, and D. S. Jin, Nature (London) **454**, 744 (2008).
- [15] P. Zhang, P. Naidon, and M. Ueda, Phys. Rev. Lett. **103**, 133202 (2009).
- [16] A. M. Kaufman, R. P. Anderson, T. M. Hanna, E. Tiesinga, P. S. Julienne, and D. S. Hall, Phys. Rev. A **80**, 050701 (2009).
- [17] T. M. Hanna, E. Tiesinga, and P. S. Julienne, New Journal of Physics **12**, 083031 (2010).
- [18] T. V. Tscherbul, T. Calarco, I. Lesanovsky, R. V. Krems, A. Dalgarno, and J. Schmiedmayer, Phys. Rev. A **81**, 050701 (2010).
- [19] D. J. Papoular, G. V. Shlyapnikov, and J. Dalibard, Phys. Rev. A **81**, 041603 (2010).
- [20] A. V. Avdeenko, Phys. Rev. A **86**, 022707 (2012).
- [21] D. Xiong, H. Chen, P. Wang, X. Yu, F. Gao, and J. Zhang, Chin. Phys. Lett. **25**, 843 (2008).
- [22] D. Xiong, P. Wang, Z. Fu, and J. Zhang, Opt. Express **18**, 1649 (2010).
- [23] D. Xiong, P. Wang, Z. Fu, S. Chai, and J. Zhang, Chin. Opt. Lett. **8**, 627 (2010).
- [24] P. Wang, L. Deng, E. W. Hagley, Z. Fu, S. Chai, and J. Zhang, Phys. Rev. Lett. **106**, 210401 (2011).
- [25] Z. Fu, L. Huang, Z. Meng, P. Wang, X. -J. Liu, H. Pu, H. Hu, and J. Zhang, Phys. Rev. A **87**, 053619 (2013).
- [26] Z. Fu, L. Huang, Z. Meng, P. Wang, L. Zhang, S. Zhang, H. Zhai, P. Zhang, and J. Zhang, Nature Phys. **10**, 110 (2014).
- [27] J. P. Gaebler, J. T. Stewart, T. E. Drake, D. S. Jin, A. Perali, P. Pieri, and G. C. Strinati, Nature Phys. **6**, 569 (2010).
- [28] K. Dieckmann, C. A. Stan, S. Gupta, Z. Hadzibabic, C. H. Schunck, and W. Ketterle, Phys. Rev. Lett. **89**, 203201 (2002).
- [29] T. Bourdel, J. Cubizolles, L. Khaykovich, K. M. F. Magalhaes, S. J. J. M. F. Kokkelmans, G. V. Shlyapnikov, and C. Salomon, Phys. Rev. Lett. **91**, 020402 (2003).
- [30] C. A. Regal, M. Greiner, and D. S. Jin, Phys. Rev. Lett. **92**, 083201 (2004).
- [31] J. L. Roberts, N. R. Claussen, S. L. Cornish, and C. E. Wieman, Phys. Rev. Lett. **85**, 728 (2000).
- [32] A. Marte, T. Volz, J. Schuster, S. Durr, G. Rempe, E. G. M. van Kempen, and B. J. Verhaar, Phys. Rev. Lett. **89**, 283202 (2002).
- [33] T. Weber, J. Herbig, M. Mark, H.-C. Nagerl, and R. Grimm, Science **299**, 232 (2003).
- [34] H. Wu and J. E. Thomas, Phys. Rev. Lett. **108**, 010401 (2012).